J Mol Model (2010) 16:771–780
DOI 10.1007/s00894-009-0582-2

ORIGINAL PAPER

Structural basis for decreased affinity of Emodin binding to Val66-mutated human CK2α as determined by molecular dynamics

Na Zhang · Rugang Zhong

Received: 4 July 2009 / Accepted: 22 August 2009 / Published online: 11 October 2009

Abstract Protein kinase CK2 (casein kinase 2) is a multifunctional serine/threonine kinase that is involved in a broad range of physiological events. The decreased affinity of Emodin binding to human CK2α resulting from single-point mutation of Val66 to Ala (V66A) has been demonstrated by experimental mutagenesis. Molecular dynamics (MD) simulations and energy analysis were performed on wild type (WT) and V66A mutant CK2α-Emodin complexes to investigate the subtle influences of amino acid replacement on the structure of the complex. The structure of CK2α and the orientation of Emodin undergo changes to different degrees in V66A mutant. The affected positions in CK2α are mainly distributed over the glycine-rich loop (G-loop), the α-helix and the loop located at the portion between G-loop and α-helix (C-loop). Based on the coupling among these segments, an allosteric mechanism among the C-loop, the G-loop and the deviated Emodin is proposed. Additionally, an estimated energy calculation and residue-based energy decomposition also indicate the lower instability of V66A mutant in contrast to WT, as well as the unfavorable energetic influences on critical residue contributions.

Keywords Binding affinity · Emodin · Hydrophobic interaction · MM/PBSA · Molecular dynamics simulations · Protein kinase CK2

N. Zhang (✉) · R. Zhong
College of Life Science and Bioengineering,
Beijing University of Technology,
Beijing 100124, China
e-mail: nanatonglei@bjut.edu.cn

Introduction

Protein kinase CK2, a multifunctional and ubiquitous eukaryotic serine/threonine kinase, is important in cellular functions, transformation and circadian rhythm, as it phosphorylates of more than 300 physiological substrates [1–3]. As such, it operates as a key switch in a myriad of physiological events and any aberrant activation of CK2 becomes an oncogenic force that underlies both the development of malignant transformation in several tissues and aggressive tumor behavior. Thus, CK2 is an attractive therapeutic target and a number of pharmacological inhibitors of this enzyme have been evaluated as promising drug candidates [4, 5].

CK2 often presents as a heterotetramer composed of two catalytic subunits (α and /or α') and two regulatory β subunits. The detailed forms of the holoenzyme are different in every species examined thus far [6, 7]. The exceptional feature of CK2α among protein kinases is its ability to use either ATP or GTP as a phosphate donor for phosphorylation. The enzyme is inhibited by inhibitors that bind to the active site of the kinase and compete for nucleotide triphosphate binding [8–10]. The ATP-competitive inhibitors of CK2α can be classified into five categories: flavonoids, hydroxylcoumarins, hydroxyantraquinones, halogenated benzimidazoles, and indoloquinazoline. Despite their structural differences and wide chemical diversity, these compound have a number of properties in common: (i) they have a low molecular weight with a rather flat and hydrophobic heterocyclic structure; (ii) all of these compounds can occupy the smaller hydrophobic pocket that is characteristic of CK2α compared to other protein kinases; (iii) the G-loop shows a variable conformation when bound to these different ligands; and (iv) structural water molecules are involved in ligand binding to CK2α.

In general, the ATP-competitive inhibitors occupy a conserved ATP-binding pocket through polar and hydrophobic interactions. For inhibitors derived from the scaffolds of Emodin and 4,5,6,7-tetrabromobenzotriazole (TBB), the main energetic contribution to binding can be principally attributed to hydrophobic interaction with the apolar surface formed by residues Leu45, Val53, Val66 (Ile in *Zea mays* CK2), Leu85, Ile95, Leu111, Phe113, Val116, Met163, and Ile174. A number of polar contacts through a polarized hydrogen bonding Lys68 and a conserved water molecule (water 1) also exists [11–15]. In addition, a large contribution to hydrophobic interactions is indicated by the linear correlation between the logKi and the accessible surface area of TBB derivatives [16] and by the linear interaction energy (LIE) model of coumarins upon binding to CK2α [17]. Inhibitory activity assays have demonstrated that CK2α has an unusually modest sensitivity to staurosporine [18], while most inhibitors show a remarkable selectivity for CK2α compared with a panel of 80 different protein kinases [19, 20]. Structure-based sequence alignment implies that there is a polar moiety somewhere in the hinge and phosphate anchor regions that include Lys68, Glu81 and Asp175 (CK2α numbering), which are quite conserved among the kinase family members. In contrast, the hydrophobic moieties have a higher degree of variability in their amino acid compositions; for example, Val(Ile)66, Met163 and Ile174 are peculiar to CK2α, as they are generally replaced with smaller ones in other protein kinases as determined from statistical analysis, (Ala versus Val66, Leu/Val versus Met163, Ala/Thr/Leu versus Ile174). The reduced dimension of the active cleft as a result of large side chain residues could account for the selectivity of inhibitors as well as for the anomalous low potency of staurosporine toward CK2α. Therefore, besides the evidently essential role of hydrophobic residues in ligand binding, some key residues in the hydrophobic portion of the binding site are also critical factors that impart the unique selectivity of inhibitors for CK2α.

The importance of the Val(Ile)66, Met163, and Ile174 residues in ligand binding has been corroborated by detailed mutational analyses [12, 13]. For example, single-point Val66 mutation to Ala in human CK2α results in a measurable decrease in IC50 of Emodin from 5.9 μM to >50 μM [18]. However, the subtle role of Val66 in ligand binding cannot be determined from this type of experiment. It is necessary to use other methods, such as molecular modeling, to further characterize the effects of amino acid substitution on the structural dynamic features of protein and ligand binding.

Molecular dynamics (MD) simulation is a well-established technique that complements experimentally determined characterizations by providing detailed dynamical behaviors of motional processes at the molecular level [21, 22]. It also allows energy calculations to be performed by the post processing method, MM/PBSA/GBSA (molecular mechanical/Poisson-Boltzmann/generalized_born surface area), which has been successfully applied to study protein-protein complexes [23] and protein-ligand affinity [24].

In the present study, molecular dynamics analysis was applied to investigate the decreased binding affinity that is observed in CK2α due to V66A mutation. Based on the implied structural features of the V66A mutant derived from MD simulations and energy calculations, an allosteric mechanism among the C-loop, G-loop, and a deviated Emodin is proposed.

Methods

System setup and parameters preparation

The atomic coordinates of the WT were directly obtained from the Protein Data Bank (PDB entry is 3BQC [25]) and hetero atoms, except for water molecules within 5.0 Å of the ligand, were removed. The V66A mutant was modeled based on the WT by replacing target residues with the desired amino acid. According to the pKa values of three hydroxyls, based on Hammett theory and their position near to residues environment, Emodin should be present, at least partially, in its mono-anionic form under the experimental pH 8.5. One of the Emodin hydroxyl groups is considered to have a formal net charge equal to −1 and to participate in the strong electrostatic interaction between Lys68 and water 1[13]. Partial charges of Emodin were obtained *via* quantum electronic structure calculations, which included use of an optimization procedure *via* the Gaussian 03 program [26] at the HF/6-31G* level, electrostatic potential (ESP) generation using Merz-Singh-Kollman van der Waals parameters [27], and the atom-centered charge fitting through the RESP [28] program implemented in the AMBER 10 package [29]. The two systems subsequently were immersed in a truncated octahedron periodic box filled with TIP3P water molecules [30] and neutralized by adding the necessary amount of Cl- ions in electrostatically preferred positions. The SANDER module with the 2003 force field reported by Duan et al. [31] was used for MD simulations.

Molecular dynamics simulations

Conventional MD simulations were initiated on the WT and V66A mutant and each simulation was performed for 7 ns. The protocol for MD simulation on two systems is as follows: (1) Optimization and relaxation were initially performed by means of several subsequent minimizations,

during which decreasing force constants were applied to the backbone atoms, and the entire system was then minimized without any constraint. (2) Each energy-minimized structure was gradually warmed to a final temperature of 300 K over 15 psec (ps), followed by constant temperature equilibration at 300 K for 35 psec with constant volume dynamics. During this step, the density of the system was stabilized. (3) Finally, constant pressure dynamics simulation was carried out on the warmed system for 5 ns, using a non-bonded cutoff of 10 Å to truncate the VDW non-bonded interactions. Temperature (300 k) and constant pressure (1 atm) were maintained by Langevin dynamics temperature coupling with a time constant of 1.0 ps [32] and isotropic position scaling with a relaxation time of 2.0 ps, respectively. The SHAKE algorithm [33], with a tolerance of 10-5, was used to constrain all bond lengths involving hydrogen atoms, while the particle-mesh-Ewald (PME) method [34] was introduced for the long-range electrostatic contribution to the force field. During the production run, 5000 structures for each simulation were saved for post processing by uniformly sampling the trajectory.

The analysis of MD simulations was carried out with the PTRAJ module. The RMSD values for CK2α CA atoms during the production phase, relative to the initial configuration, were monitored and taken as a measure of whether the MD trajectories were or were not stable. Snapshots for energy analysis were obtained from the last 1000 ps, at 10 ps intervals.

MM/PBSA and MM/GBSA calculations

The binding energy of the CK2α-Emodin complex was calculated using MM/PBSA single trajectory methodology [35, 36] according to

$$\Delta G_{binding} = G_{complex} - G_{protein} - G_{ligand} = \Delta E_{MM} + \Delta G_{sol} - T\Delta S,$$

where ΔE_{MM} is the molecular mechanics interaction energy, comprised of electrostatic energy and van der Waals energies. It was calculated using the sander without applying a cutoff for non-bonded interactions. The solvation free energy (ΔG_{sol}) was estimated by continuum solvent methods as the sum of electrostatic (ΔG_{polar}) and non-polar ($\Delta G_{nonpolar}$) contributions. ΔG_{polar} was calculated by solving the Poisson-Boltzmann equations with a grid spacing of 0.4 Å, and the values of interior dielectric constant and exterior dielectric constant were set to 1 and 80, respectively. The non-polar component ($\Delta G_{nonpolar}$), as a linear function of solvent-accessible surface area (SASA), was represented as $\Delta G_{nonpolar}=\lambda SASA+b$, where $\lambda=0.00542$ kcalÅ−2 and b=0.92 kcal mol^{-1} [37]. The time-consuming conformational entropy change, -TΔS, was not considered because of the large computational overhead and low prediction accuracy [38, 39]. We have also neglected the entropy term, assuming that it will be very similar for all of the systems. Thus, the energy we calculated is not a true binding free energy. Apart from the calculation of relative binding affinities, a per-residue decomposition of the total energy using the MM/GBSA decomposition process was also performed to evaluate the contribution of each residue to the binding in each of the two systems. Here, the polar contribution of desolvation was computed using the GB model [40]. The detailed theory of energy decomposition is described elsewhere [41].

Results

To elucidate the structural effects of a V66A substitution, we chose to focus on the structural changes of CK2α, on the interactions between Emodin and CKα, and on the coupling among the C-loop, the G-loop, and the reoriented Emodin.

Global structural features

The time-dependent root-mean-square deviation (RMSD) profiles from the starting structure for WT and V66A mutant are displayed in Fig. 1. A convergent behavior during the last 1000 ps simulation time indicates that acceptable equilibrium states are being approached. The RMSD average values of CK2α remain at about 1.7 Å and 2.5 Å for WT and the V66A mutant, respectively, suggesting that the structure of V66A CK2α undergo conformational changes to some degree. In the case of Emodin, due to its rigid structure characteristics, the RMSD values of Emodin in the two systems have an overlapping range from 0.1 to 0.2 Å during the entire course of simulation, with an average of 0.15 Å in the equilibration period. Each system in equilibrium has stabilized sufficiently for sampling to be statistically valid.

To estimate the dynamic flexibility of the regions in the protein structure, the residue fluctuations characterized by B-factors are plotted in Fig. 2. Judging from the higher B-factor values in the region of the G-loop and C-loop for V66A CK2α, these residues appear to exhibit abnormal behaviors in the enzymatic function of CK2α. The detailed changes could be deduced from structural superimpositions. The WT average structure shows the relative whole-translation movement in contrast to the starting configuration (Fig. 3) without any observable changes. For the V66A mutant, by superimposing the averaged structures of both systems, remarkable structural changes can be clearly seen, which mainly distribute over the G-loop and C-loop in V66A CK2α, especially in the

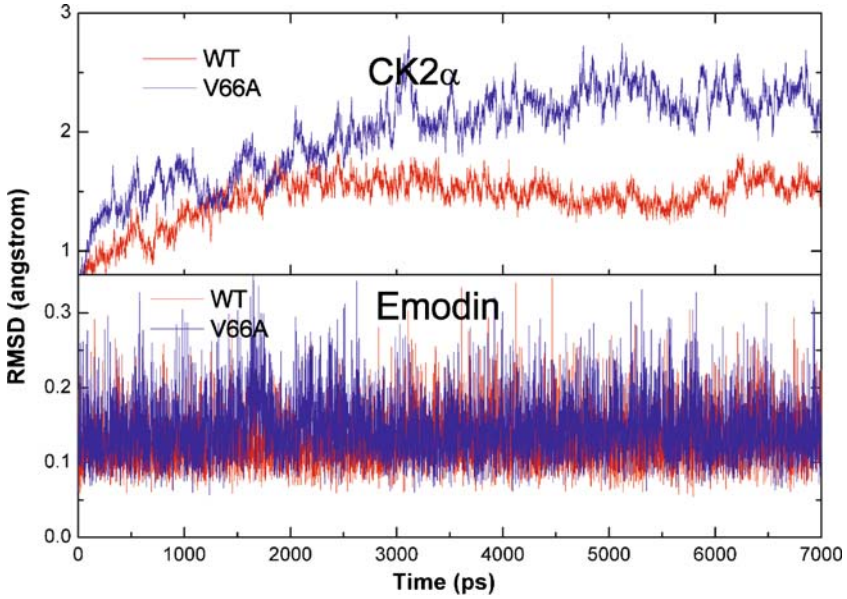

Fig. 1 The time-dependent RMSD for CK2α (upper panel) and ATP (lower panel) for WT (red) and V66A mutant (blue)

"open" conformation of G-loop. This is in agreement with the conformational state of the G-loop in *apo* CK2, in contrast to that in the presence of Emodin, as demonstrated by experimental analysis. Here, the notable change in the G-loop is the orientation of the tip residue Tyr50, which is nearly vertical to that in the WT.

Interestingly, our previous studies have revealed that the equivalent residue, either Phe67 in GSK3β [22] or Tyr15 in CDK2 [42], also plays a vital role in anchoring the proper conformation of the G-loop. As the functional role of the G-loop is to correct the alignment of the ATP phosphate moiety for the catalytic reaction [43, 44], the G-loop in an "open" state definitely affects the orientation of Emodin, a feature that could not have been deduced from the stable RMSD values. The detailed structural features of Emodin, the C-loop and the G-loop will now be discussed.

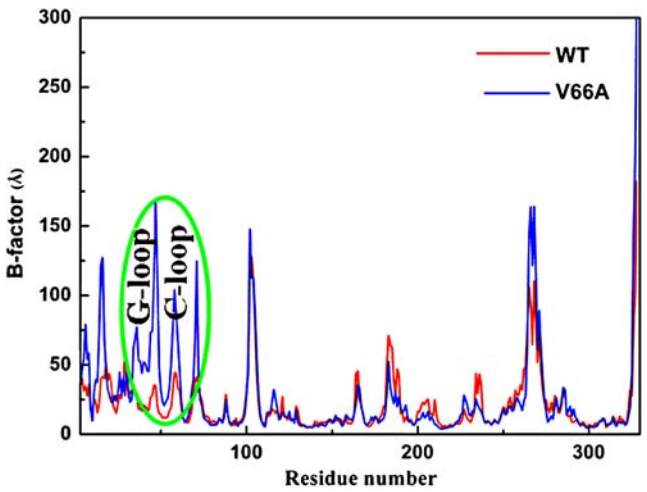

Fig. 2 The calculated per residue B-factor for CK2α between WT (red) and V66A mutant (blue)

Different Emodin binding modes

The binding mode of Emodin with CK2α in the WT simulation is extremely similar to that determined from its crystallographic structure. Emodin locates at the active site of the enzyme and binds primarily through hydrophobic and polar interactions (Fig. 4). A hydrophobic cavity consisting of Leu45, Val53, Val66, Ile95, Phe119, Met163, and Ile174 accommodates the aromatic rings of Emodin. Additionally, a number of polar interactions involving conserved water 1, Lys68, Glu81, and Asp175 contribute to anchoring the orientation of Emodin. The O4 atom of Emodin forms electrostatic interactions with the side chain of Ly68 and conserved water 1. A statistical analysis finds that water 1 is highly conserved in 20 CK2α structures and it plays essential functions in ligand binding and in stabilizing protein structure. Simultaneously, the water 1 participates in electrostatic interaction networks involving residues Lys68, Glu81 and Asp175. Strong electrostatic interaction networks formed between these three amino acids (Fig. 5) are located at left and forward of Emodin, respectively. Therefore, the orderly hydrophobic and polar interactions position Emodin into the CK2α active pocket.

Emodin in the V66A mutant, although locates in the co-substrate binding cavity of CK2α, displays a position and orientation that is quite different from that in WT, and the aforementioned interactions disappear. As shown in Fig. 6, the aromatic rings extend into the portion of the nucleotide-binding cleft. Here, they are encompassed by Val53, Ile95,

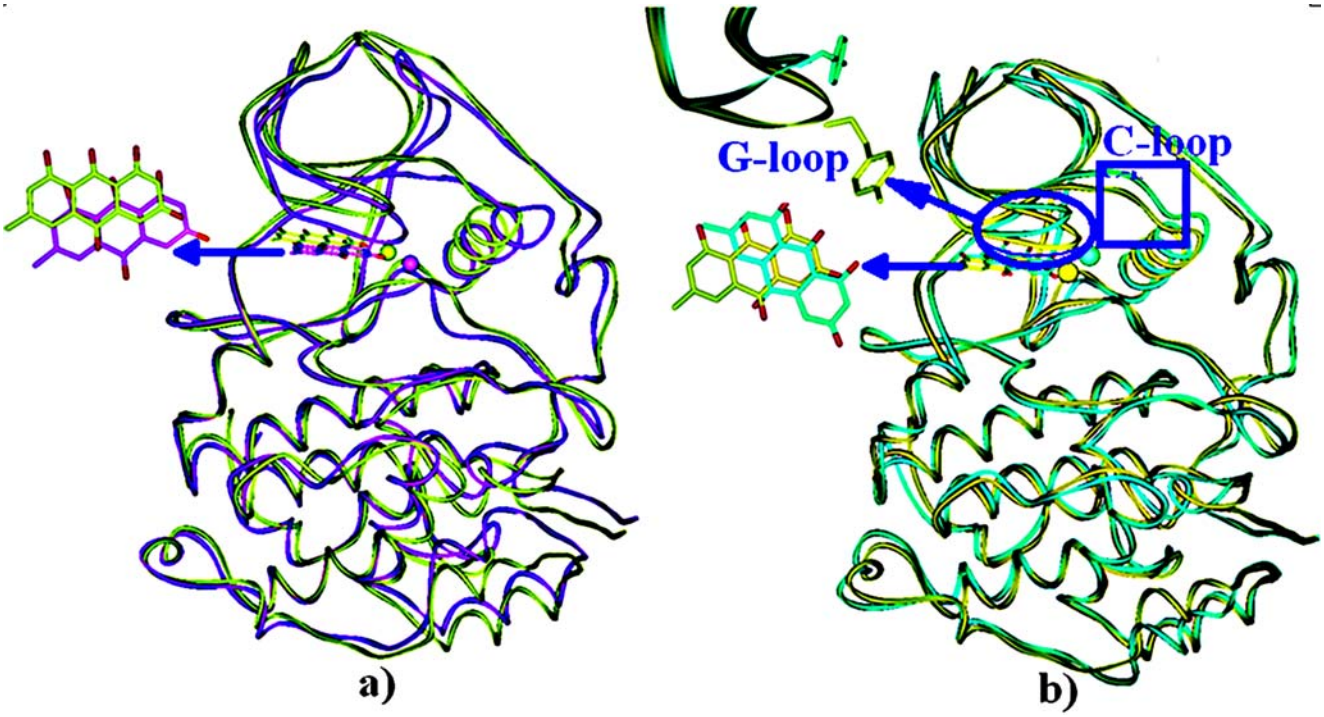

Fig. 3 The overall structural comparison (**a**) between averaged structure (yellow) and starting configuration (purple); (**b**) between WT (yellow) and V66A mutant (cyan)

Phe119, and Ile174, whereas the Ala66 and Met163 almost make no contact with Emodin. Thus, the residue replacement generates a packing defect at the hydrophobic interface. In terms of the electrostatic interactions, the O4 atom still interacts with the side chain atom of Lys68, and the conserved water 1 still serves as a hydrogen-bonding bridge between the O5 atom and the side chain oxygen atom of Glu81. In contrast, the electrostatic interactions between Lys68 and Glu81 appear to be weakened, with intermittent existence, as well as the complete loss of ion-pairing between Lys68 and Asp175. Improper relative positions and orientation of Emodin and CK2α indicate that these interactions are not as specific or orderly as those seen in the WT.

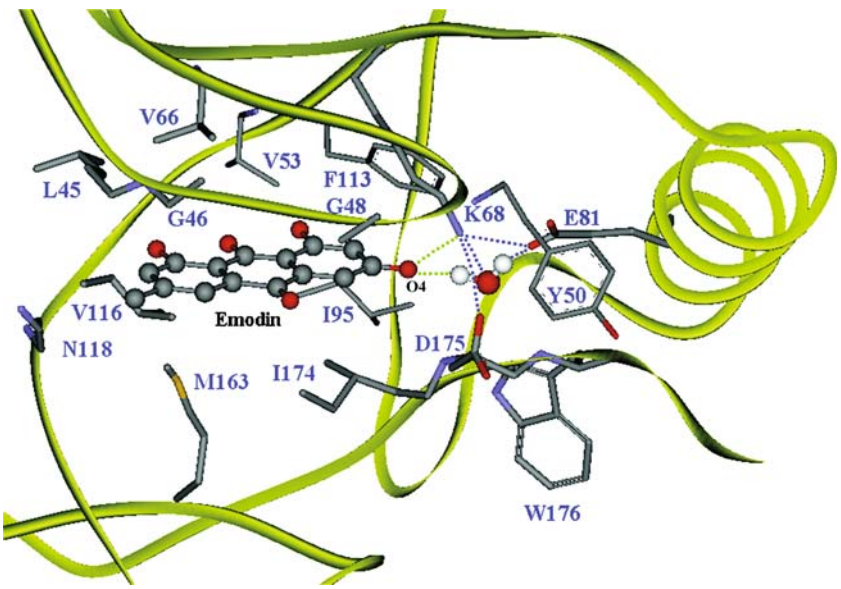

Fig. 4 The stable interactions between Emodin and CK2α of WT. The key residues of CK2α are shown in stick with element colors, and the Emodin atoms are represented as ball and stick

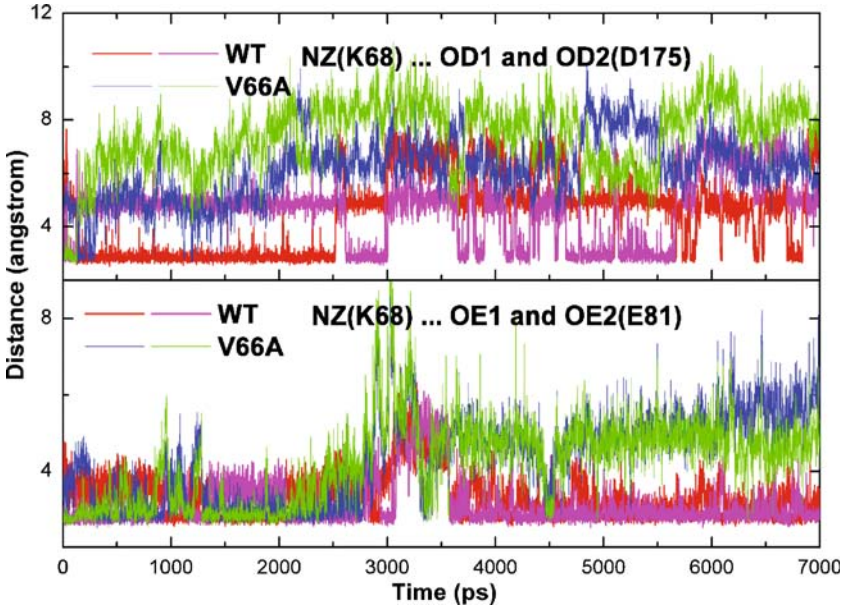

Fig. 5 Time evolution of distances between NZ atoms of Lys68 and OE1 and OE2 atoms of Glu81 (lower panel), and OD1 and O2 atoms of Asp175 (upper panel) for WT (red and magenta) and V66Amutant (blue and green)

As stated above, the volume reduction from the residue Val to Ala results in a hydrophobic packing defect in the binding interface and a high flexibility of the C-loop. This induces the G-loop to deviate away from its original position, which in turn impairs the orderly binding of Emodin with CK2α. The detailed coupling between C-loop and G-loop will be discussed next.

Energy analysis

The different interaction modes provide a full description of the two complexes, while binding energy calculations provide the qualitative analysis for the effects of residue replacement on ligand binding affinity. The MM/PBSA energy terms presented in Table 1 illustrate the lower binding affinity of the V66A mutant relative to the WT. The ΔE_{ele} values of the V66A mutant exhibit a ~2 kcal mol^{-1} more unfavorable value than that of WT complex, which is in agreement with the loss of salt bridges between Lys68 and Glu81 and Asp175 in the V66A mutant. The $\Delta\Delta G_{subtotal}$ can be crudely approximated at 7.17 kcal mol^{-1} and is in accordance with the instability of the V66A mutant derived from qualitative analysis.

To evaluate the energetic influences on the contributions of critical residues, modeling of the residue-based energy decomposition of the interaction energy between CK2α and Emodin was performed (Fig. 7). Major favorable energy contributions ranging from −6 to −1 kcal mol^{-1} originate predominantly from Leu45,

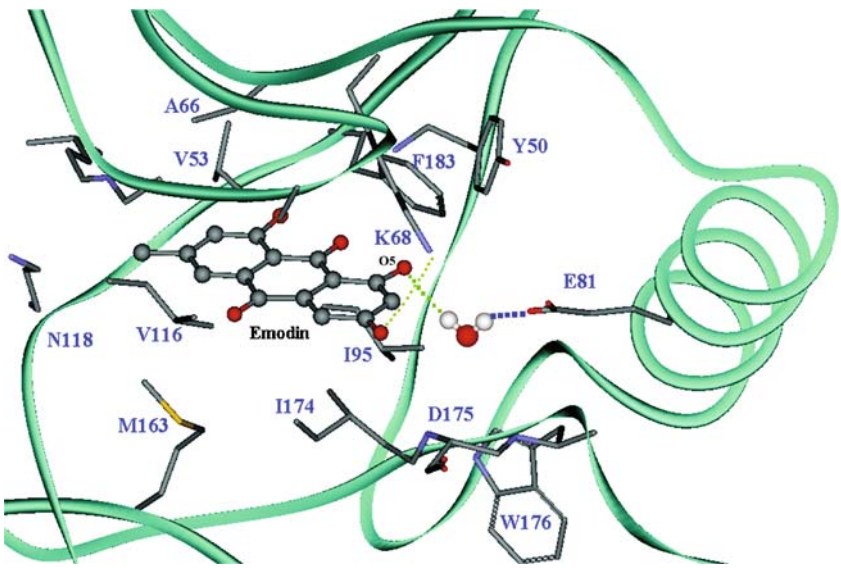

Fig. 6 The position and orientation of Emodin locating at binding pocket of V66A mutant

Table 1 Energy terms of MM/PBSA results for WT and V66A mutant complexes

Energy terms[a]	WT	V66A
ΔE_{ele}	−82.22	−80.34
ΔE_{vdw}	−31.44	−35.27
ΔE_{MM}	−113.66	−115.62
ΔG_{polar}	−4.29	−4.51
$\Delta G_{nonpolar}$	89.79	99.14
ΔG_{sol}	85.50	94.63
$\Delta G_{subtotal}$	−28.16	−20.99
$\Delta\Delta G_{subtatal}$	0	7.17

[a] $\Delta E_{MM} = \Delta E_{vdw} + \Delta E_{ele}, \Delta G_{subtotal} = \Delta E_{MM} + \Delta G_{sol}$

Val53, Val66, Lys68, Glu81, Ile95, Phe113, Met163 and Ile174, which is consistent with dominant roles for these amino acids in the electronic and hydrophobic interactions in WT. In the V66A mutant, however, the energy values of most of the corresponding residues increase to different extents compared with those of the WT, especially Leu45, Val66, Lys68 and Met163, creating a ~2.0 kcal mol^{-1} change of more unfavorable energy to the total energy. These data agree with the loss of hydrophobic contacts and electronic interactions of critical residues, as described in the MD simulation results.

The coupling among the C-loop, the G-loop, and the reoriented Emodin

The C-loop and G-loop display remarkable structural changes when superimposed upon an average structure of the two enzymes. Here, the relative conformation of the α-helix, C-loop, and G-loop is coupled by several interactions, including the hydrophobic interactions between Phe54 of the G-loop and Ile69 of the C-loop, between aromatic ring of Tyr50 of the G-loop and Val73 of the C-loop, and ion pairing between Lys68 of C-loop and Glu81 of the α-helix (Fig. 8). However, a hydrophobic interaction between Tyr50 and Val73 exists in the shifted C-loop and the "open" G-loop of the V66A mutant, as well as a weakened ion-pairing between Lys68 and Glu81. Perhaps due to the unanchored C-loop that occurs due to the presence of Ala66, the flexible C-loop allows the Lys68 to shift away from the side chain of Glu81 and Asp175. This is followed by a deviation of the C-loop away from the G-loop, and the hydrophobic force between Tyr50 and Val73 may then compel the subsequent reorientation of Tyr50 side chains, leaving it nearly vertical to its original orientation in the WT. Consequently, the "open" conformation of G-loop is unfavorable for interacting with Emodin. And also our previous study has elucidated the crucial roles of the salt bridges network between Lys85 and Glu97 and Asp200 (corresponding to Lys68, Glu81, and Asp175 in CK2, respectively) in stabilizing the structure of active GSK3β [45].

A similar coupling mechanism between the C-loop and the G-loop is also found to interpret the loss of catalytic activity of a cAMP-dependent protein kinase (PKA) that lacks phospho-Thr197 [46], as well as inactive GSK3β due to Arg96 mutation [22]. In addition, within the protein kinase family, a conserved aromatic residue, tyrosine or phenylalanine (corresponding to Tyr50), is usually found as @ in the G-loop motif GXGX@G. Since the aromatic side chain caps the site of phosphate transfer, this site has been focused on as a target of drug design and generates large structural

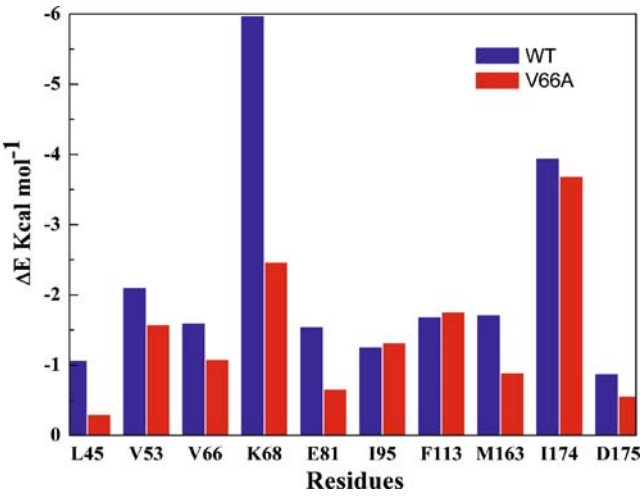

Fig. 7 The residue-based energy decomposition on critical residues of WT (red) and V66A mutant (blue)

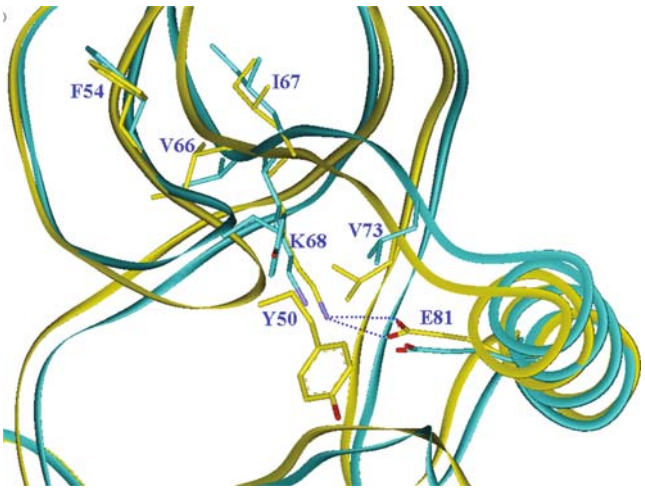

Fig. 8 The coupled interactions between C-loop and G-loop in WT (yellow) and V66A mutant (cyan). Important residues are shown in stick modes with the O and N atoms in element color

distortions in the loop upon interaction with some inhibitors [47, 48].

Discussion

The importance of hydrophobic residues such as Met163 and Ile174 in ligand binding has been well documented by the effects of either single point mutation or of combined mutations on inhibitor binding affinity [11]. Per-residue energy decomposition indicates the dominant contributions of these residues for ligand binding, which further confirms their functional roles. The V66A mutation decreases the binding affinity of Emodin by destabilizing the protein structure, by destroying the integrity of hydrophobic cavity and subsequently by inducing a deviant orientation of Emodin. These conclusions are supported by other experimental MD analyses that have reported similar results. For example, Niefind et al. [49] has elucidated the structural characteristics of a human double mutant V66A/M163L CK2α in a complex with AMPPNP by comparing with the structure of Zea mays CK2 and wild type human CK2 [50]. Features such as observable changes in the G-loop, flexibility of the α-helix, and the considerable deviations in the purine plane and in the phosphate group of AMPPNP were reported, which are similar to those reported in the present study for the structure of the V66A mutant. In addition, Tyr50 is coordinated by Lys74 and Lys77 in active human CK2α in a complex with AMPPNP [50], whereas the anchoring of Tyr50 by these two residues is destroyed in the V66A mutant and in the inactive human CK2α structure [51].

Besides the significance of Val66 and Ile174 in ligand binding, the key roles of two residues that modulate the target selectivity to CK2α should also be mentioned. A series of 70 Quinobene analogues exhibit a remarkable inhibitory power toward CK2 with IC_{50} values of <2 μM. In contrast, the IC_{50} value for TBB inhibition of CK2 is approximately 10-fold weaker affinity than that seen for CDK2, GSK3β, or PKA. The unique selectivity of TBB to Zea mays CK2 is attributed to the substitution of Val66 and Ile174, which are by Ala31 and Ala144 in CDK2. Consequently, the ATP binding pocket shape of CK2, as measured by molecular surface area, is smaller than that of CDK2, and TBB in CDK2 is rotated and placed more toward the hinge region compared with TBB placement in Zea mays CK2 [52].

Conclusions

Molecular dynamics simulations and energy analysis were conducted to explore instability of V66A CK2α-Emodin complex. The V66A mutation results in a packing defect due to a change in hydrophobicity and also creates an abnormal behavior of the G-loop, the α-helix, and the C-loop. The changes in coupling of these portions of the enzyme induce a deviation in the positioning of Emodin. An allosteric pathway among the C-loop, G-loop, and deviated Emodin is proposed. Improper relative positions and orientations of Emodin within the V66A CK2α could explain the decreased affinity of Emodin binding to CK2α. Energy analysis also provides a qualitative explanation of the energetic effects of substitution of Val66 by Ala on the binding affinity between CK2α and Emodin.

Acknowledgments This work was funded by China Postdoctoral Science Foundation funded project (No. 20090450271) and Beijing Natural Science Foundation (8072006). We acknowledge Professor David Case for the kind gift of AMBER 10 software.

References

1. Litchfield DW (2003) Protein kinase CK2: structure, regulation and role in ellular decisions of life and death. Biochem J 369:1–15
2. Duncan JS, Litchfield DW (2008) Too much of a good thing: The role of protein kinase CK2 in tumorigenesis and prospects for the therapeutic inhibition of CK2. Biochim Biophys Acta 1784:33–47
3. Meggio F, Pinna LA (2003) One-thousand-and one substrates of protein kinase CK2? FASEB J 17:349–368
4. Ahmad KA, Wang G, Slaton J, Unger G, Ahmed K (2005) Targeting CK2 for cancer therapy. Anticancer Drugs 16:1037–1043
5. Unger GM, Davis AT, Slaton JW, Ahmed K (2004) Protein kinase CK2 as regulator of cell survival: implications for cancer therapy. Curr Cancer Drug Targets 4:77–84
6. Bibby AC, Litchfield DW (2005) The multiple personalities of the regulatory subunit of protein kinase CK2: CK2 dependent and CK2 independent roles reveal a secret identity for CK2 beta. Int J Biol Sci 1:67–79
7. Pinna LA (2002) Protein kinase CK2: a challenge to canons. J Cell Sci 115:3873–3878
8. Mazzorana M, Pinna LA, Battistutta R (2008) A structural insight into CK2 inhibiton. Mol Cell Biochem 316:57–62
9. Prudent R, Cochet C (2009) New protein kinase CK2 inhibitors: Jumping out of the catalytic box. Chem Biol 16:112–120
10. Niefind K, Putter M, Guerra B, Issinger OG, Schomburg D (1999) GTP plus water mimic ATP in the active site of protein kinase CK2. Nat Struct Bio 6:1100–1103
11. Battistutta R, Sarno S, De Moliner E, Papinutto E, Zanotti G, Pinna LA (2000) The replacement of ATP by the competitive inhibitor Emodin induces conformational modifications in the catalytic site of Protein kinase CK2. J Bio Chem 275:29618–29622
12. Sarno S, Sali M, Battistutta R, Zanotti G, Pinna LA (2005) Features and potentials of ATP-site directed CK2 inhibitors. Biochim Biophys Acta 1754:263–270
13. Battistutta R, De Moliner E, Sarno S, Zanotti G, Pinna LA (2001) Structural features underlying selective inhibition of protein kinase CK2 by ATP site-directed tetrabromo-2-benzotriazole. Protein Sci 10:2200–2206

14. De Moliner E, Moro S, Sarno S, Zagotto G, Zanotti G, Pinna LA, Battistutta R (2003) Inhibition of protein kianse CK2 by Anthraquinone-related compounds. J Biol Chem 278:1831–1836
15. Battistutta R, Mazzorana M, Cendron L, Bortolato A, Sarno S, Kazimierczuk Z, Zanotti G, Moro S, Pinna LA (2007) The ATP-binding site of protein kinase CK2 holds a positive electrostatic area and conserved water molecules. Chembiochem 8:1804–1809
16. Battistutta R, Mazzorana M, Sarno S, Kazimierczuk Z, Zanotti G, Pinna LA (2005) Inspecting the structure-activity relationship of protein kinase CK2 inhibitors derived from tetrabromobenzimidazole. Chem Biol 12:1211–1219
17. Chilin A, Battistutta R, Bortolato A, Cozza G, Zanatta S, Poletto G, Mazzorana M, Zagotto G, Uriarte E, Guiotto A, Pinna LA, Meggio F, Moro S (2008) Coumarin as attractive casein kinase 2 (CK2)inhibitor scaffold: an integrate approach to elucidate the putativebinding motif and explain structure-activity relationships. J Med Chem 51:752–759
18. Sarno S, Moro S, Meggio F, Zagotto G, Dal Ben D, Ghiselline P, Battistutta R, Zanotti G, Pinna LA (2002) Toward the rational design of protein kinase casein kinase-2 inhibitors. Pharmacol Ther 93:159–168
19. Pagano MA, Bain J, Kazimierczuk Z, Sarno Stefania S, Ruzzene M, Di Maira G, Elliott M, Orzeszko A, Cozza G, Meggio F, Pinna LA (2008) The selectivity of inhibitors of protein kinase CK2: an update. Biochem J 415:353–365
20. Sarno S, Vaglio P, Meggio F, Ruzzene M, Davies SP, Donella Deana A, Shugar D, Pinna LA (2001) Selectivity of 4, 5, 6, 7-terabromobenzotriazole, an ATP-site-directed inhibitor of protein kinase CK2 ('casein kinase-2'). FEBS Lett 496:44–48
21. Zhang N, Jiang YJ, Zou JW, Zhuang SL, Jin HX, Yu QS (2007) Insights into unbinding mechanisms upon two mutations investigated by molecular dynamics study of GSK3β-Axin complex: Role of packing hydrophobic residues. Proteins 67:941–949
22. Zhang N, Jiang YJ, Zou JW, Zhao WN, Yu QS (2009) Structural basis for the complete loss of GSK3β catalytic activity due to R96 mutation investigated by molecular dynamics study. Proteins 75:671–681
23. Gohlke H, Case DA (2004) Converging free energy estimates: MM-PB(GB)SA studies on the protein-protein complex Ras-Raf. J Comput Chem 25:238–250
24. LepšíK M, Kříž Z, Havlas Z (2004) Efficiency of a second generation HIV-1 protease inhibitor studied by molecular dynamics and absolute binding free energy calculations. Proteins 57:279–293
25. Raaf J, Klopffleisch K, Issinger O-G, Niefind K (2008) The catalytic subunit of Human protein kinase CK2 structurally deviates from Its maize homologue in complex with the nucleotide competitive inhibitor Emodin. J Mol Biol 377:1–8
26. Frisch MJ, Trucks GW, Schlegel HB, Scuseria GE, Robb MA, Cheeseman JR, Zakrzewski VG, Montgomery JA Jr, Stratmann RE, Burant JC, Dapprich S, Millam JM, Daniels AD, Kudin KN, Strain MC, Farkas O, Tomasi J, Barone V, Cossi M, Cammi R, Mennucci B, Pomelli C, Adamo C, Clifford S, Ochterski J, Petersson GA, Ayala PY, Cui Q, Morokuma K, Malick DK, Rabuck AD, Raghavachari K, Foresman JB, Cioslowski J, Ortiz JV, Stefanov BB, Liu G, Liashenko A, Piskorz P, Komaromi I, Gomperts R, Martin RL, Fox DJ, Keith T, Al-Laham MA, Peng CY, Nanayakkara A, Gonzalez C, Challacombe M, Gill PMW, Johnson BG, Chen W, Wong MW, Andres JL, Head-Gordon M, Replogle ES, Pople JA (2003) Gaussian 03, Revision C.02. Gaussian Inc, Wallingford, CT
27. Besler BH, Merz KM, Kollman PA (1990) Atomic charges derived from semiempirical methods. J Comput Chem 11:431–439
28. Fox T, Kollman PA (1998) Application of the RESP methodology in the parametrization of organic solvents. J Phys Chem B 102:8070–8079
29. Case DA, Darden T, Cheathem TE III, Simmerling C, Wang JM, Duke RE, Luo R, Merz KM, Wang B, Pearlman DA, Croley M, Brozell S, Tsui V, Gohleke H, Mongan J, Hornak V, Cui GL, Beroza P, Schafmeister C, Caldwell JW, Ross WS, Kollman PA (2008) AMBER 10. University of California, San Francisco
30. Jorgensen WL, Chandrasekhar J, Madura JD, Impey RW, Klein ML (1983) Comparison of simple potential functions for simulating liquid water. J Chem Phys 79:926–935
31. Duan Y, Wu C, Chowdhury S, Lee MC, Xiong G, Zhang W, Yang R, Cieplak P, Luo R, Lee T (2003) A point-charge force field for molecular mechanics simulations of proteins. J Comput Chem 24:1999–2012
32. Berendsen HJC, Postma JPM, van Gunsteren WF, Di Nola A, Haak JR (1984) Molecular dynamics with coupling to an external bath. J Chem Phys 81:3684–3690
33. Ryckaert JP, Ciccotti G, Berendsen HJC (1977) Numerical integration of the cartesian equations of motion of a system with constraints:molecular dynamics of n-alkanes. J Comput Phys 23:327–341
34. Darden T, York D, Pedersen L (1993) Particle mesh Ewald: an N log $^{(N)}$ method for Ewald sums in large systems. J Chem Phys 98:10089–10094
35. Massova I, Kollman PA (2000) Combined molecular mechanical and continuum solvent approach (MM-PBSA/GBSA) to predict ligand binding. Persp Drug Discov Des 18:113–135
36. Kollman PA, Massova I, Reyes C, Kuhn B, Shuanghong H, Chong L, Lee M, Lee T, Duan Y, Wang W, Donini O, Cieplak P, Srinivasan J, Case DA, Cheatham TE III (2000) Calculating structures and free energies of complex molecules: Combining molecular mechanics and continuum models. Acc Chem Res 33:889–897
37. Sitkoff D, Sharp KA, Honig B (1994) Accurate calculation of hydration free energies using macroscopic solvent models. J Phys Chem 98:1978–1988
38. Wang W, Kollman PA (2001) Computational study of protein specificity: The molecular basis of HIV-1 protease drug resistance. Proc Natl Acad Sci USA 98:14937–14942
39. Wang J, Morin P, Wang W, Kollman PA (2001) Use of MM-PBSA in reproducing the binding free energies to HIV-1 RT of TIBO derivatives and predicting the binding mode to HIV-1 RT of efavirenz by docking and MM-PBSA. J Am Chem Soc 123:5221–5230
40. Jayaram B, Sprous D, Beveridge DL (1998) Solvation free energy of biomacromolecules: parameters for a modified generalized born model consistent with the AMBER force field. J Phys Chem B 102:9571–9576
41. Gohlke H, Kiel C, Case DA (2003) Insights into protein-protein binding by binding free energy calculation and free energy decomposition for the Ras-Raf and Ras-RalGDS complexes. J Mol Biol 330:891–913
42. Welburn JP, Tucker JA, Johnson T, Lindert L, Morgan M, Willis A, Nobe MEM, Endicott JA (2007) How Tyrosine 15 phosphorylation inhibits the activity of Cyclin-dependent kinase 2-cyclin A. J Biol Chem 282:3173–3181
43. Aimes RT, Hemmer W, Taylor SS (2000) Serine-53 at the tip of the glycine-rich loop of cAMP-dependent protein kinase: role in catalysis, P-site specificity, and interaction with inhibitors. Biochem 39:8325–8332
44. Grant B, Hemmer W, Tsigelny I, Adams JA, Taylor SS (1998) Kinetic analyses of mutations in the glycine-rich loop of cAMP-dependent protein kinase. Biochemistry 37:7708–7715
45. Sun H, Jiang YJ, Yu QS, Luo CC, Zou JW (2008) Effect of mutation K85R on GSK-3β: Molecular dynamics simulation. Biochem Biophys Res Commun 377:962–965

46. Jin HX, Wu TX, Jiang YJ, Zou JW, Zhuang SL, Mao X, Yu QS (2007) Role of phosphorylated Thr-197 in the catalytic subunit of cAMP-dependent protein kinase. J Mol Struct 805:9–15
47. Schindler T, Bornmann W, Pellicena P, Miller WT, Clarkson B, Kuriyan J (2000) Structural mechanism for STI-571 inhibition of abelson tyrosine kinase. Science 289:1938–1942
48. Mohammadi M, McMahon G, Sun L, Tang C, Hirth P, Yeh BK, Hubbar SR, Schlessinger J (1997) Structures of the tyrosine kinase domain of fibroblastgrowth factor receptor in complex with inhibitors. Science 276:955–960
49. Niefind K, Yde CW, Ermakova I, Issinger OG (2007) Evolved to be active: Sulfate ions define substrate recognition sites of CK2α and emphasise its exceptional role within the CMGC family of eukaryotic protein kinases. J Mol Biol 370:427–438
50. Yde CW, Ermakova I, Niefind K (2005) Incling the purine base binding plane in protein kinase CK2 by exchanging the flanking side-chains generates a preference for ATP as a cosubstrate. J Mol Biol. 347:399–414
51. Raaf J, Issinger OG, Niefind K (2009) First inactive conformation of CK2α, the catalytic subunit of protein kinase CK2. J Mol Biol 386:1212–1221
52. De Moliner E, Brown NR, Johnson LN (2003) Alternative binding modes of an inhibitor to two different kinases. Eur J Biochem 270:3174–3181